Proceedings Paper:

Ball, E.A. orcid.org/0000-0002-6283-5949 (2021) Investigation into the relationship between conversion gain, local oscillator drive level and DC bias in a SiGe transistor transconductance modulated mixer at 24-28 GHz. In: 2021 IEEE Texas Symposium on Wireless and Microwave Circuits and Systems (WMCS). 2021 IEEE Texas Symposium on Wireless and Microwave Circuits and Systems, 18-20 May 2021, Waco, TX, USA (Virtual conference). IEEE (Institute of Electrical and Electronics Engineers) . ISBN 9781665431392

https://doi.org/10.1109/WMCS52222.2021.9493227

Investigation into the Relationship Between Conversion Gain, Local Oscillator Drive Level and DC Bias in a SiGe Transistor Transconductance Modulated Mixer at 24-28 GHz

Edward A. Ball
Communications Research Group, The University of Sheffield, UK
e.a.ball@sheffield.ac.uk

Abstract— **In this paper a model is presented to predict RF mixer conversion gain as a function of the Local Oscillator (LO) drive level and DC bias, for a transconductance modulated mixer. From this, the possibility to trade-off LO RF power and DC bias to achieve a desired conversion gain is identified. Analytical model results, simulation results and measured data from a hardware prototype are presented.**

Index Terms—**Mixers, transconductance modulation, bipolar transistor circuits, millimeter wave circuits.**

I. Introduction

There is now much interest in the 28 GHz mmWave band, triggered by worldwide 5G activity. The use of this band for 5G, 6G and beyond will increase and so there is a clear need for power-efficient and cost-effective solutions for RF hardware implementations. RF mixers are a vital part of a radio system and the need for a downconverting mixer operating at 24-28 GHz with a 5 GHz intermediate frequency (IF), hence a local oscillator (LO) range of 19-23 GHz is the basis of the research reported in this paper.

Generation of LO power at carrier frequencies above 10 GHz is expensive in terms of circuit complexity and consumed DC power. Therefore, it is important to try and minimize the LO power required by a mixer for a desired target RF performance. This paper investigates the viability of trading LO RF power with DC bias in a single transistor transconductance modulated mixer. As part of the analysis, an analytical model to predict the IF current generated by the mixing operation within the transistor is developed, leading to a prediction of IF conversion gain.

Published techniques exploring transistor mixer conversion gain have focused on fixing the DC bias and varying LO power for best performance [1]-[3] but have not extensively jointly explored the trade-off between both DC bias and LO drive. Diode mixers are also popular [4] but usually require higher LO drive powers. Many integrated mixers use the well-known Gilbert Cell mixer strategy [5], [6], requiring several transistors. However, at mmWave frequencies, there is much attraction in simple circuit concepts that are reliable and power-efficient whilst using few active devices. This becomes even more important when operating beyond mmWave frequencies. Downconversion mixers at mmWave frequencies and higher now use SiGe [7], [8]; GaAs [9], [10] and other advanced materials such as InP, often focusing on FET devices. The concepts in the paper are demonstrated using a commercial SiGe bipolar junction transistor (BJT) but are semiconductor material agnostic.

II. Model for BJT Collector Current

To allow a practical analysis to be conducted, a commercial transistor was selected as the basis of the investigation. The proposed transistor was a SiGe BJT BFP740FH6 from Infineon Ltd, with a transition frequency of 45 GHz. The first step in predicting the achievable conversion gain is to understand the device I-V characteristics at DC and then at the centre frequency of the LO, 21 GHz. Fig. 1 shows a plot of the vendor-provided spice model subject to a DC *Vbe* sweep along with the extracted data from a simple Keysight ADS simulation for DC and AC operation. AC operational testing measured the peak collector AC current *Ic* amplitude for a peak AC *Vbe*.

Fig. 1 shows the achieved *Ic* vs *Vbe* for an AC signal driving the base produces a reduced peak collector current, compared to DC tests (due to device parasitics). Note this is not simply an offset in the exponential 'knee' but also a reduction of the achieved transconductance at lower collector currents. To investigate how to model this effect, the parameters for a Gummel-Poon representation of the BJT were tuned to get an improved fit to the AC data. Even then, the Gummel-Poon model still has notable error around the knee, so an alternative parametric fitting model was sought. A dual exponential model (1) was found to give a closer fit to the extracted simulated AC data.

$$I_C(Vbe) = a.e^{b.Vbe} + c.e^{d.Vbe} \tag{1}$$

In (1) the coefficients were selected for least squares best fit to the ADS AC data and were: a = -4.35e-22 A, b = 42.76 V^{-1}, c = 9.20e-08 A, d = 13.45 V^{-1}. It was noted experimentally that the accuracy of fitting the waveform around the knee was particularly important for predicting the *Ic* IF currents.

978-1-6654-0309-2/21/$31.00 ©2021 IEEE

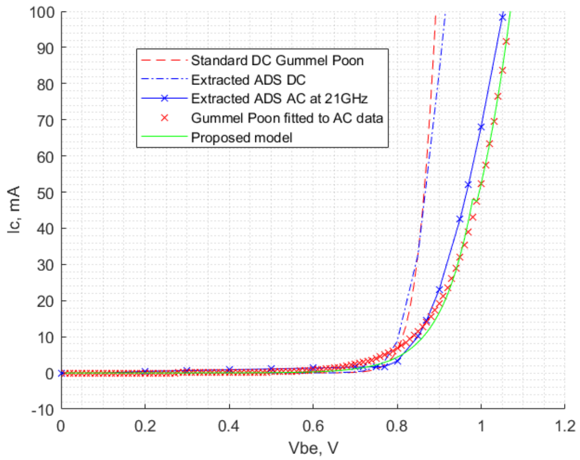

Fig. 1. Comparison of DC *Ic* vs *Vbe* and AC *Ic* vs *Vbe* for different models.

The selected *Ic* model reverts from (1) to the tuned Gummel-Poon model for *Vbe* > 0.98 V.

In general, let the base drive voltage *Vbe* consists of 3 components: a DC bias *Vb*, the LO drive of form $Al.\cos(\omega_L.t)$ and the incoming RF signal $Ar.\cos(\omega_R.t)$, combined as shown in (2).

$$Vbe = Vb + Al.\cos(\omega_L.t) + Ar.\cos(\omega_R.t) \qquad (2)$$

III. Modelling IF Transconductance Mixing Current

The BJT non-linear *Ic*-*Vbe* curve will produce a mixing component at an IF and it is desirable to be able to predict this transconductance mixing current. The aim is to develop a relationship between DC base bias *Vb* and LO base amplitude *Al* and the resulting IF current amplitude (and hence mixer conversion gain).

In modelling the mixer conversion gain, a simple useful technique is to assume the *Ic* due to the large LO drive produces a clipped cosine waveform [11], [12]. Assuming such a cosine model for the collector current is of the form $Ipk.cos(\theta)$ where θ is the LO phase over 1 cycle, *Ipk* is the peak *Ic* (due to in-phase alignment of *Vb* and *Al*) and then calculating the DC and fundamental Fourier coefficients from the time domain *Ic* waveform, the equivalent sinusoidal collector current at the LO (*C1*) and the equivalent DC current (*C0*) can be found. However, as *Vb* is decreased and *Al* increased significantly, the current waveform is better modelled in the form $Ipk.cos(2\theta)$ which then requires modification to the models for *C1* and *C0*. To span the two extreme states, an adaptable definition for *C0* and *C1* is needed that represents the time domain *Ic* waveform. The time domain representation of this improved fit model are (3), (4), (5), where parameter *k* is used to fit the model to a time domain current profile.

$$I_C = Ipk.cos\left(\frac{2.k.\pi.t}{T_p}\right) \text{ for } t = 0...T1 \qquad (3)$$

$$I_C = Ipk.cos\left(2\pi[1-k] + \frac{2.k.\pi.t}{T_p}\right) \text{ for } t = (Tp - T1) ... Tp \qquad (4)$$

$$I_C = 0 \text{ for } t = T1 ... (Tp - T1) \qquad (5)$$

Parameter *Tp* is the period of the LO cycle and *T1* corresponds to the point where the collector current has fallen to a negligible value (i.e. transistor *Vbe* below approx. 0.75 V), measured from cycle time *t* = 0. The Fourier coefficients for the resulting DC *C0* and *C1* 1st harmonic currents are then represented by (6), (7) and (8).

$$C_0 = \frac{I_{pk}}{2k\pi}\left[sin\left(\frac{2k\pi T_1}{T_p}\right) - sin\left(2\pi - \frac{2k\pi T_1}{T_p}\right)\right] \qquad (6)$$

$$C_{1k} = \frac{Ipk}{4\pi}\left\{\frac{2\sin\left[\frac{2\pi T_1(k+1)}{Tp}\right]}{k+1} + \frac{2\sin\left[\frac{2\pi T_1(k-1)}{Tp}\right]}{k-1}\right\} \qquad (7)$$

When *k* =1, (14) is used.

$$C_{1k} = Ipk\left\{\frac{\sin\left[\frac{4\pi T_1}{Tp}\right]}{4\pi} + \frac{T_1}{T_p}\right\} \qquad (8)$$

The *k* value required is a function of *Al/Vb* and is initially found via simulation, as will be discussed later. Fig. 2 shows an example collector current waveform from models (3), (4), (5) compared with the extracted AC collector current model (1), for a given combinations of *Al* and *Vb*. The improved fit for the $cos(k\theta)$ model can be seen. Critical model parameter time value *T1* can be approximated by (9).

$$T_1 = \frac{T_p}{2\pi}\cos^{-1}\left(\frac{I_{bm}}{I_{bm}-I_{pk}}\right) \qquad (9)$$

Parameter *Ibm* is the current due only to *Vb* using (1), with no applied AC signal.

The optimal value of *k* for a given *T1* and *Tp* is found using (10), where *m* and *f* are linear parameters for a simple straight-line model dependent on ratio *Al/Vb*, found via simulation to obtain an acceptable fit between (1) versus (3), (4), (5) over the bias range to be investigated.

$$k = \frac{A_L}{V_b}.m + f \qquad (10)$$

As *Vb* is increased, so does background DC collector current *Ibm*, which has the effect of reducing *C1*. This effect can be included in the *C1* model by (11).

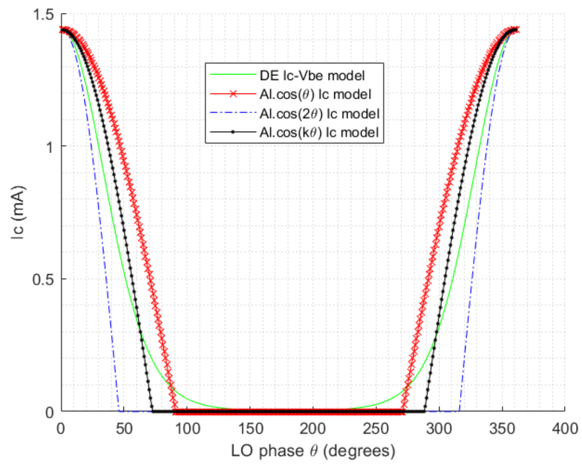

Fig. 2. Time domain collector current profiles for models $cos(\theta)$, $cos(2\theta)$, $cos(k\theta)$ (LO *Al* = 0.22 V, *Vb* = 0.6 V).

$$C_{1'} = C_1 - \frac{I_{bm}}{\pi}\left[sin\left(\frac{2\pi T_1}{T_p}\right)\right] \tag{11}$$

Using the models for *Ic* with chosen bias *Vb* and LO level *Al*, the transconductance due to LO drive and hence *C1* can be represented by (12).

$$gm_{LO} = \frac{2.C_{1'}}{A_L} \tag{12}$$

From (12) it is then possible to consider the transconductance modulated by the LO to mix with an input RF signal and hence produce the desired IF current component, where $Ar.\cos(\omega_R)$ is the RF signal entering the mixer.

$$I_{mix} = Ar.\cos(\omega_R)\,.\,gm_c.\cos(\omega_{LO}) \tag{13}$$

Following trigonometric expansion and assuming only the lower frequency mixing product is of interest, we arrive at a prediction for the IF current available at the collector (14), where the conversion transconductance gm_C is half of gm_{LO}.

$$I_{IF} = A_R.gm_c.cos([\omega_R - \omega_R]t) \tag{14}$$

Hence (14) is now a prediction of the IF current due to the collector current LO waveform, ignoring any device physical current limiting mechanisms.

A. LO Peak Current Limitation

The analytical model thus far does not include mechanisms to limit the peak current as will be present in a practical device. The boundary of the saturation region defines a curve for *Vce* and *Ic*. A transistor cannot sustain a *Vce* below the *Vce(sat)* at a particular current. By reducing the *Ipk* value to a lower value that jointly satisfies the *Vce(sat)* boundary for *Ic* and the resulting *Vce* for the current when injected into the collector's matching network impedance, a simple revised limiting value of current can be found and used for *Ipk*. (This revised limit value of *Ipk* need only be used when the *Vce* calculated for a given value of peak LO current would fall below the permitted *Vce(sat)* for the device at that current.)

B. Effect of Bias Change on Device Input and Output Match

It is proposed that *Ic* consisting of a fixed DC current and a Fourier DC component *C0*, resulting from the LO current waveform, could be represented by a single equivalent DC current. Simulations of the resulting S22 have confirmed this concept is valid – a similar S22 is achieved when the BJT is LO pumped as if a fixed DC bias of the same *C0* value was applied.

As the LO drive *Al* or bias *Vb* change, the DC current and *C0* will change from the target design value (where the transistor's input and output match have been designed), so there will be a reduction in IF current available, due to the S11 (RF) an S22 (IF) effective match change. This can be modelled by evaluating the device input reflection coefficient using the bias-dependent S parameters and LO short circuit load on the collector, as required for good mixer operation. A base mismatch effect can then be modelled by considering a potential divider as the base input network, with a driving source impedance chosen to be the conjugate of the transistor's input impedance at the target bias. Thus, as *C0* changes and hence the bias changes, the RF level presented at the base will change due to the implicit impedance change in the base. A similar simple model is developed for effective gain reduction on the output, due to S22 changes from *C0*. This is implemented in the model as a scaling to *C1* that depends on *C0*, as shown in (15).

$$C_{1r} = C_{1'}[C_0.m\_S + f\_S] \tag{15}$$

In (15) *m_S* and *f_S* were pre-calculated based on a perceived insertion loss change at the base and collector as the bias point changes, using the vendor's S parameters, resulting in *m_S* = -6.0 A^{-1} and *f_S* = 1.1 for the BFP740F.

IV. Mixer Trial Circuit

To allow a comparison with the above analytical models, a Keysight ADS circuit simulation was created for the SiGe transistor mixer. The target LO range was 19-23 GHz and the RF range 24-28 GHz.

Rogers RO4003C substrate was used (0.5 mm thick, ε_r of 3.55, loss tangent of 0.0027).

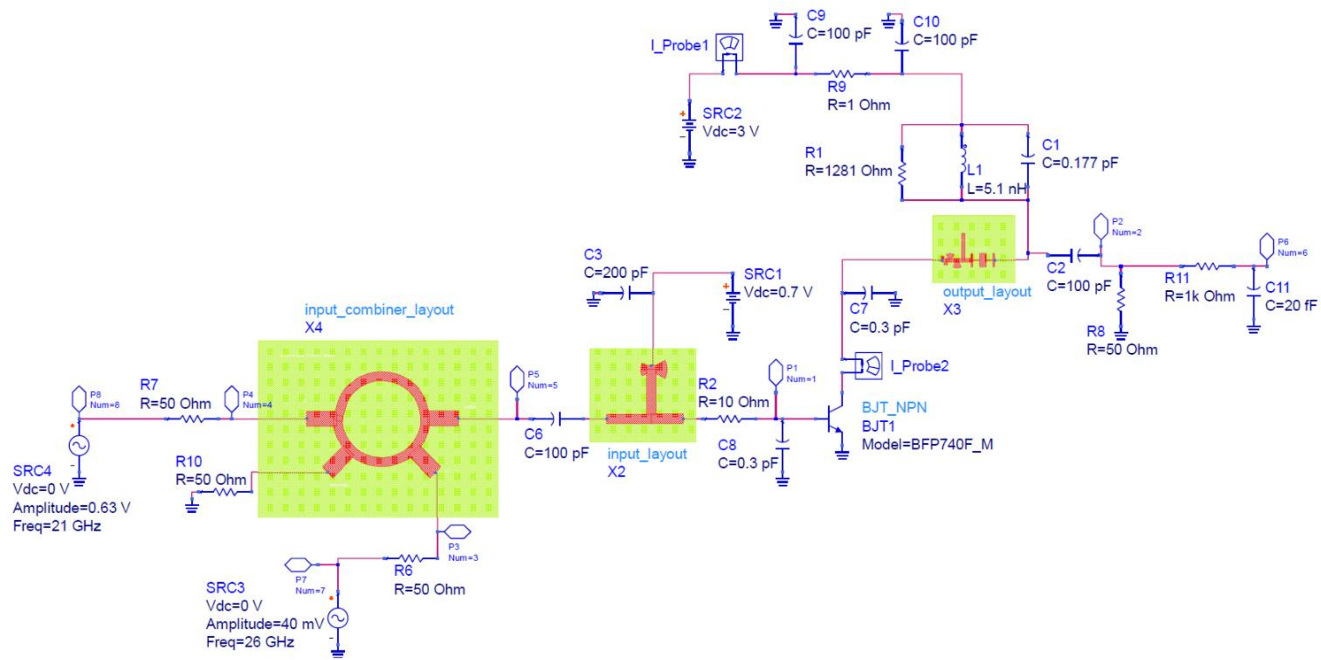

Fig. 3. BJT mixer ADS simulation circuit.

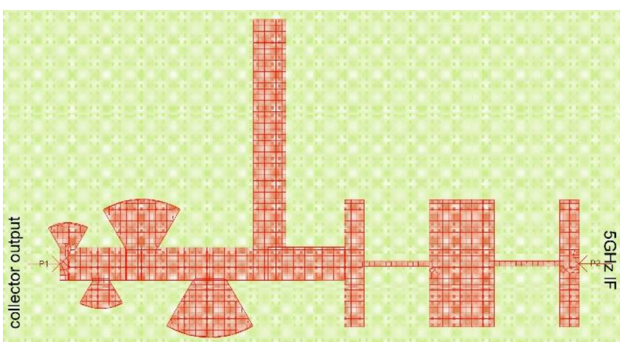

Fig. 4. Mixer output LO suppression, match and LPF network.

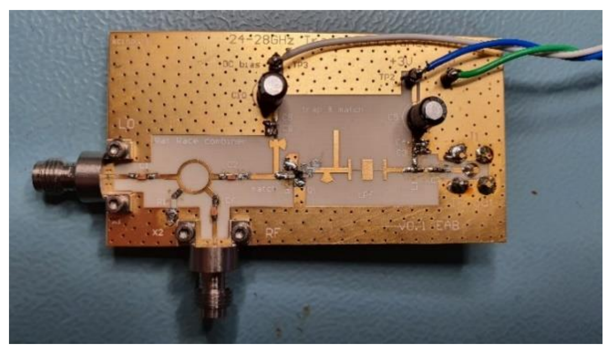

Fig. 5. Built BFP740FH6 24-28 GHz mixer prototype.

The simulated circuit is shown in Fig. 3. The input RF and LO signals are combined and isolated using a rat-race and then passed through a conjugate matching network that feeds the base. The collector network consists of radial stubs to suppress the LO and its second harmonic, followed by an IF matching network and LPF, as shown in Fig. 4. To further test the concept, a 26 GHz mixer on PCB was implemented using the developed design. During testing, as the transistor is biased with increasingly higher DC currents, care must be taken to ensure the device remains stable. A small value resistor in the base feed helps maintain stability, if required. The assembled mixer PCB is shown in Fig. 5.

V. Comparison between Analytical Model and Circuit Simulation

A Matlab simulation was created of the analytical models, to explore different values of bias *Vb* and LO drive *Al* on IF current generation, with a fixed RF level *Ar*.

The extracted IF currents in Fig. 6 show the results from tests comparing the ADS circuit simulator and the analytical models. The possibility to trade DC bias *Vb* for LO power to achieve a given IF current (and hence conversion gain) can be seen. The realizable IF current limit is defined by the onset of *Vce(sat)* for the +10dBm LO drive and the effect of (11). The discrepancy between the analytical model and simulated circuit in Fig. 6 can be seen to consist of two aspects: *Vb* alignment and peak IF current overestimation. The *Vb* realignment required is circa 50 mV at +10 dBm LO. It is proposed that this error is minor, given the simple nature of the model. The overestimation of the peak IF current is suspected to be due to the techniques in III.A for representing peak *Ic*.

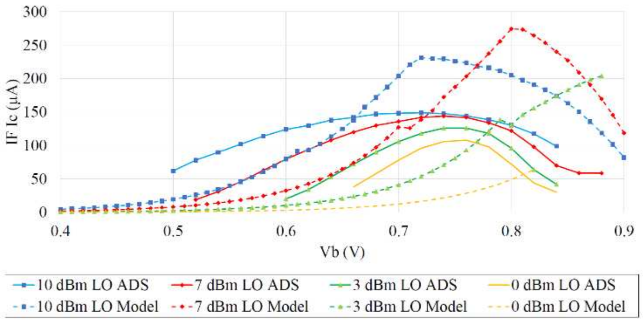

Fig. 6. Comparison of model IF currents and ADS simulation for BFP740 mixer (LO powers: +10 / +7 / +3 / 0 dBm).

However, it is proposed that the trend of IF current vs *Vb,* up to peak current and accounting for the *Vb* offset, is represented by the model. Also, after accounting for the *Vb* offset, the location of the peak current in the model aligns well with the measured peak. The model also captures the tailing off of IF current for higher *Vb* with high LO powers.

A. *Exploration of Performance as a Function of LO Drive and DC Bias*

Using the analytical models (AMs), DC bias *Vb* was swept from 0 to 0.9 V and amplitude *Al* swept from 0 to 0.9 V, with *Ar* fixed. The available surface of transconductance mixer IF currents is shown in Fig. 7. To account for the limited accuracy of the analytical models at higher IF currents (as seen in Fig. 6) the IF currents above 200 μA are not shown on Fig. 7. Two interesting features of Fig. 7 are *1)* the sharp upper boundary tracing around high *Vb* over a range of *Al* and *2)* the ridge appearing to show optimum *Al* and *Vb* pairings for operation below peak IF current. The upper limit maximum IF current boundary shows a complicated relationship between *Vb* and *Al*, but with a zone around *Vb* = 0.8 V and *Al* = 0.25 V for an area of maximum gain.

From the above analysis, the general concept of being able to trade *Al* and *Vb* appears to be valid, though the relationship between them needs to be developed further.

VI. Hardware Prototype Mixer Test results

A BFP740F hardware prototype mixer was built, based on the simulated design, to explore the achievable performance and trade-offs.

The LO and RF input signals are combined using a rat-race. This also serves the purpose of isolating the RF port from the LO port. The measured LO – RF isolation was better than 20 dB for LOs between 20 – 23 GHz.

Testing investigated the effect of adjusting *Vb* on the conversion gain achieved for an LO at 21 GHz with drive powers of 10 dBm, 7 dBm, 3 dBm and 0 dBm. The RF signal was set to 26 GHz at -20 dBm, resulting in a 5 GHz IF.

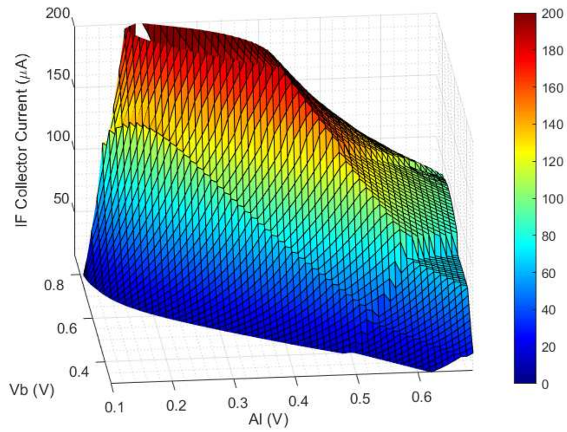

Fig. 7. Analytical model transconductance IF current surface.

TABLE I
MIXER CONVERSION GAIN WHEN *Ic* FIXED CLOSE TO 10 MA DC

***Vb* (V)**	**LO Drive (dBm)**	**Conversion Gain: Measured** [ADS / AMs] **(dB)**	**DC Current: Measured** [ADS / AMs] **(mA)**
0.67	+10	**-11.3** [-9.0 / -5.0]	**11.0** [11.5 / 13.0]
0.77	+3	**-14.3** [-10.2 / -8]	**10.1** [11.3 / 10.3]
0.79	0	**-19.0** [-13.5 / -15.9]	**11.0** [12.0 / 7.5]

The first test adjusted *Vb,* with LO applied, to achieve a circa 10 mA operating DC draw, with example measured, simulated and model conversion gains shown in TABLE I. This test showed that simply defining a fixed DC draw current and adjusting *Vb* and *Al* to achieve this draw will not result in a constant gain across the bias scenarios.

Tests then investigated sweeping *Vb* for each LO drive level and measuring the resulting conversion gain. A trade-off between the LO drive and *Vb* for a desired conversion gain was observed (as predicted by Fig. 6) and seen in Fig. 8. TABLE II identifies the optimum value of *Vb* for maximum conversion gain. By comparing TABLE I and TABLE II there is a benefit seen in adjusting *Vb* to optimise the conversion gain for each LO drive. By using this approach with the 0 dBm LO drive, the conversion gain of -19 dB can be improved to -12.8 dB whilst reducing the DC current draw from 11 mA to 3.2 mA. Also, to achieve a conversion gain of -11.3 dB requires 10 dBm LO in TABLE I but only +3 dBm LO for -11.6 dB gain in TABLE II. It is interesting to note that the peak measured gain for *Vb* of 0.61 V and +10 dBm LO power (0.3 V *Al* at the base) aligns with the IF current ridge on Fig. 7. The DC current models are close to measurements.

The measured PCB mixer with *Vb* from Table II had an input P1dB (P1dBi) of +6 dBm for a +10 dBm LO and +1 dBm P1dBi for a +3 dBm LO. As is common, this shows the higher LO drive is providing improved linearity. This can be important and offers the possibility to optimise *Vb* and LO power for a given gain / P1dBi requirement.

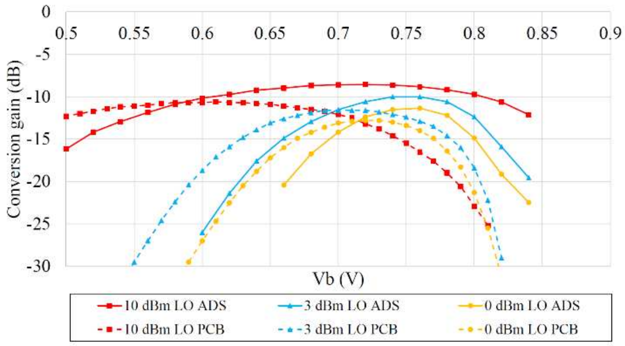

Fig. 8. Measured & ADS simulated mixer conversion gain as function of *Vb* and LO power (LO powers: +10 / +3 / 0 dBm).

TABLE II
MIXER CONVERSION GAIN EXAMPLES WITH *VB* OPTIMIZED

***Vb* (V)**	**LO Drive (dBm)**	**Conversion Gain Measured** [ADS / AMs] **(dB)**	**DC Current Measured /** [ADS / AMs] **(mA)**
0.61	+10	**-10.6 (peak)** [-10.1 /-9.3]	**6.3** [6.8 / 8.5]
0.72	+3	**-11.6 (peak)** [-10.6 /-13.9]	**4.4** [4.9 / 5.2]
0.73	0	**-12.8 (peak)** [-11.9 / -23.0]	**3.2** [3.6 / 3.3]

The prototype conversion gain achieved is negative largely due to losses in the input rat-race and network feeding the transistor base. By using the ADS simulation and calculating the conversion gain with respect to the applied base voltage (rather than the rat-race input port), the conversion gains shown in TABLE III are anticipated.

TABLE III
MIXER CONVERSION GAIN REFERRED TO BASE INPUT (ADS)

***Vb* (V)**	**LO Drive (dBm)**	**Simulated Conversion Gain (dB)**
0.68	+10	+2.0
0.76	+3	-0.1
0.76	0	-1.5

VII. CONCLUSION

In this paper it is shown that the IF current (and hence the conversion gain) that can be achieved from a SiGe BJT 24-28 GHz mixer can be approximated using simple mathematical analytical models. A key finding is that for operation below peak conversion gain, LO drive power can be traded against *Vb* bias for a given gain, whilst also providing savings in required LO power. These concepts allow RF front-end mixers to be dynamically reconfigured for a particular operational gain scenario, especially where modest P1dBi reduction can be tolerated. Models are validated with simulation results and test results from a manufactured transconductance mixer.

ACKNOWLEDGMENT

This work was in part supported by a UKRI Future Leaders Fellowship [grant number MR/T043164/1].

REFERENCES

[1] Y. Yan, M. Bao, S. E. Gunnarsson, V. Vassilev, and H. Zirath, "A 110-170-GHz multi-mode transconductance mixer in 250-nm InP DHBT technology," *IEEE Transactions on Microwave Theory and Techniques*, vol. 63, no. 9, pp. 2897–2904, Sep. 2015, doi: 10.1109/TMTT.2015.2459676.

[2] X. Ning, H. Yao, X. Wang, and Z. Jin, "A W-band single-ended downconversion / upconversion gate mixer in InP HEMT technology," in *Proceedings of ICMTCE 2013 - 2013 IEEE International Conference on Microwave Technology and Computational Electromagnetics,* 2013, pp. 277–279, doi: 10.1109/ICMTCE.2013.6812434.

[3] R. A. Pucel, D. Masse, and R. Bera, "Performance of GaAs MESFET mixers at X band," *IEEE Trans. on Microwave Theory and Techniques*, vol. 24, no. 6, pp. 351–360, Jun. 1976.

[4] C. Wang, D. Hou, J. Chen, and W. Hong, "A dual-band switchable MMIC star mixer," *IEEE Microwave and Wireless Components Letters*, vol. 29, no. 11, pp. 737–740, Nov. 2019, doi: 10.1109/LMWC.2019.2940637

[5] Y. Zhang et al., "12-mW 97-GHz low-power downconversion mixer with 0.7-V supply voltage," *IEEE Microwave and Wireless Components Letters*, vol. 29, no. 4, pp. 279–281, Apr. 2019, doi: 10.1109/LMWC.2019.2901410.

[6] H. D. Yen, J. S. Yuan, G. W. Huang, W. K. Yeh, and F. S. Huang, "Reliability performance of a 70-GHz mixer in 65-nm technology," *IEEE Transactions on Device and Materials Reliability*, vol. 16, no. 1, pp. 101–104, Mar. 2016, doi: 10.1109/TDMR.2016.2523881.

[7] A. Guner, T. Mausolf, J. Wessel, D. Kissinger, and K. Schmalz, "A 440-540-GHz subharmonic mixer in 130-nm SiGe BiCMOS," *IEEE Microwave and Wireless Components Letters*, vol. 30, no. 12, pp. 1161–1164, Dec. 2020, doi: 10.1109/LMWC.2020.3030315.

[8] Y. Jin, J. R. Long, and M. Spirito, "A 7dB NF 60GHz-band millimeter-wave transconductance mixer," *Proceedings of IEEE Radio Frequency Integrated Circuits Symposium*, 2011, pp. 1-4, doi: 10.1109/RFIC.2011.5940650.

[9] T. T. Nguyen, K. Fujii, and A. V. Pham, "Highly linear distributed mixer in 0.25-μm enhancement-mode GaAs pHEMT technology," *IEEE Microwave and Wireless Components Letters*, vol. 27, no. 12, pp. 1116–1118, Dec. 2017, doi: 10.1109/LMWC.2017.2750071

[10] T. T. Nguyen, A. Riddle, K. Fujii, and A. V. Pham, "Development of wideband and high IIP3 millimeter-wave mixers," *IEEE Transactions on Microwave Theory and Techniques*, vol. 65, no. 8, pp. 3071–3079, Aug. 2017, doi: 10.1109/TMTT.2017.2669042.

[11] S. A. Maas, *Nonlinear Microwave and RF Circuits,* 2nd ed., Norwood, USA: Artech House, 2003.

[12] D. M. Pozar, *Microwave Engineering*, 4th ed., New Jersey, USA: Wiley, 2012.